2024-01-3053 Published 08 Sep 2024

# Application of Machine Learning Models to Enable Virtual Development of High Performance Brake Systems

**David Antanaitis** General Motors LLC

***Citation:*** Antanaitis, D., "Application of Machine Learning Models to Enable Virtual Development of High Performance Brake Systems," *SAE Int. J. Advances & Curr. Prac. in Mobility* 7(3):1340-1354, 2025, doi:10.4271/2024-01-3053.

This article was presented at the Brake Colloquium & Exhibition – 42nd Annual, September 15-18, 2024.

Received: 19 Apr 2024 Revised: 28 May 2024 Accepted: 16 Jul 2024

## Abstract

The once rarified field of Artificial Intelligence, and its subset field of Machine Learning have very much permeated most major areas of engineering as well as everyday life. It is already likely that few if any days go by for the average person without some form of interaction with Artificial Intelligence. Inexpensive, fast computers, vast collections of data, and powerful, versatile software tools have transitioned AI and ML models from the exotic to the mainstream for solving a wide variety of engineering problems. In the field of braking, one particularly challenging problem is how to represent tribological behavior of the brake, such as friction and wear, and a closely related behavior, fluid consumption (or piston travel in the case of mechatronic brakes), in a model. This problem has been put in the forefront by the sharply crescendo-ing push for fast vehicle development times, doing high quality system integration work early on, and the starring role of analysis-based tools in enabling this strategy. Focusing even further, brake corner systems under duress – such as high temperatures, and high braking power, can exhibit highly non-linear and in-stop varying behavior that can be exceedingly difficult to model accurately. The present work chronicles efforts by the author and colleagues to develop machine learning models that capture this complex behavior and generalize sufficiently well to continue representing the performance of the brake under high energy driving conditions, even as the models are presented with new braking conditions that were not part of the training of the models. The utility of the models in the prediction of system-level performance is demonstrated through a case study application to calibrating a fade warning feature. The present work is shown from the perspective of a practicing engineer, not a data scientist, with some details that may prove mundane to the latter – but a strong motivation behind this work is to share the experience of getting started and some practical lessons learned towards the use of these powerful machine learning tools to solving practical problems in the field of brake engineering.

## Introduction

About 15 years ago, inspired in no small part by the very insightful, yet very approachable work of Barber [1], the author and colleagues integrated neural-network models representing the pressure to torque conversion and the fluid consumption of brake corners into a full brake system model [2]. This model was in turn integrated into a vehicle dynamics model (CarSim™) and used successfully to represent brake system performance on a racetrack. The vehicle level performance predictions with the higher fidelity brake corner models were very different from, and ultimately more realistic, than modeling based on much simpler lookup tables. As promising as this work was, it was ultimately not developed further at the time, mainly because the much easier to use lookup table models were "good enough" to make the right design decisions.

At the time of this initial research, the prevailing brake system actuation technology was vacuum boosted hydraulic brakes, with the operation of the service braking system mostly mechanical and electronic features intervening to provide slip and directional control (traction, antilock braking, and stability control features). State of the art brake actuation technology in the present is fully by-wire, with the driver pressing the brake pedal against a pedal feel simulator, sensor and control algorithms interpreting this input and translating into motor and hydraulic plunger control to generate pressure and fluid displacement. With this technology, new features to recognize severe brake fade and inform the driver, and also to detect and communicate issues such as brake fluid boil and failures in the brake system such as hydraulic leaks, becomes critical. There is a rapidly growing need based on compressed vehicle development timelines and fewer pre-production vehicle builds to develop and calibrate these features using non-vehicle based resources, such as Hardware In the Loop (HIL), Software In the Loop (SIL), and math-based simulation. Successfully developing and

calibrating an ever-growing list of brake-based features and having them work well by the time they are first operated in a new vehicle program creates a new demand for higher fidelity models of the brake system, in particular, of the brake corners where the physics of operation remain dominated by extremely complex tribology. This provided a strong impetus to re-visit and improve upon the earlier research. The new goal – a brake system model representing brake corner output and fluid consumption with enough fidelity to facilitate the calibration and integration of a "fade warning" algorithm. This was a starting point and the scope of the present research – the potential applications of such models is virtually boundless.

For the benefit of the reader and author alike, the paper is organized into the following sections:

1. The physics of brake fade and fade warning algorithms
2. Brake Corner Modeling – raw data
3. Brake Corner Model Training and Validation
4. Validation with new braking conditions
5. System model and model predictions
6. Conclusions and next steps

## 1. Physics of Brake Fade and Fade Warning Algorithms

Broadly, the term "brake fade" can be described as changes in friction, compliance, and wear as the brake system gets hot. It is experienced by the driver of an automobile as changes in brake pedal feel and potentially as dramatically shortened life of the brake friction material and/or its counter face (usually a disc). At a tribological level, brake fade involves complex physical and chemical processes. As brake fade takes hold, binder materials such as phenolic resin pyrolyze and decompose, releasing entrained particles comprising the friction material as wear debris [3]. Structural materials at the surface of the friction material, such as metal fibers and metal or ceramic chips can weaken, lose support, tear out, and fracture. Surface asperities of the brake disc can weaken, fatigue, and fracture. The third body tribofilm, enriched with a heavy flow of wear debris, can become highly dynamic, either thinning out and allowing wear to greatly accelerate, or becoming very thick and compacted, forming an accretion colloquially known as "glazing"[4,5].

The brake corner subsystem – comprised of a brake caliper, inner and outer pad assemblies, brake disc, wheel bearing, suspension or steering knuckle, and various sensors, shields and fasteners – converts the displacement of brake fluid under pressure to brake torque (see figure 1).

As brake fade sets in and the coefficient of friction between the pads and the disc decreases, and as the brake pads develop taper wear which decreases the

**FIGURE 1** High performance brake corner with aluminum 6-piston caliper two-piece cast iron disc

mechanical efficiency of the caliper [8], the amount of brake torque produced for a given pressure will drop, in turn requiring higher pressure to achieve the same torque (and therefore the desire level of deceleration). Concurrently, the brake friction material loses compressive stiffness with increasing temperature, and uneven wear of the pad such as taper wear and cupping wear under the pistons, as well is shifting of the center of pressure further away from the caliper bridge, further decrease the effective stiffness of the system. The combination of needing higher pressure to achieve a target level of braking torque, and the need to force a larger volume of fluid into the brake corner to reach this pressure, can manifest in significantly higher brake system operating pressures and fluid displacement to reach a target torque (such as that required to use all available tire traction to reduce speed prior to a sharp turn on a racetrack).

At a system level, this means the brake actuation needs to generate the higher pressure and fluid displacement. With vacuum boosters, the brake pedal the driver actuates has a direct mechanical path through to the main cylinder. Any increase in the fluid displacement needed to pressurize the brake system translates directly into increased pedal travel. Increased pressure needed translates into a roughly proportional increase in pedal force, as long as there is sufficient vacuum in the booster to provide assist. It is common for the demand for braking pressure during extremely strenuous driving conditions to exceed the capability of the vacuum booster for providing under boosted conditions [9]; this is exacerbated by the decrease in booster vacuum as pedal stroke increases. When this occurs, additional brake pressure can be generated so long as there is additional stroke remaining in the primary cylinder, but substantially higher pedal effort will be required as the ratio of output to input force drops from a boosted level (typically in the 7-10 range) down to an unboosted level (below 1).

With modern electro-hydraulic brake systems with emulated pedal feel, the brake pedal is not directly coupled to plunger that provides pressure to the downstream brake corners; therefore, the increase in fluid consumption is not directly felt. The effect of higher pressures needed will be felt to the extent that is allowed by the calibration of the system.

Figure 2 shows a previous generation high performance sport sedan with a vacuum booster, running a flat track test designed to match the braking severity of specific closed circuit, high speed trace tracks. Average brake pedal forces and travels are plotted against initial brake rotor bulk temperature and corrected to a target of 1.0g of deceleration. Data are also shown for a newer generation version of the same vehicle, equipped with an electro-hydraulic brake system with a pedal feel simulator. The newer generation vehicle is also more powerful, which drove the higher temperatures.

The data of figure 2 show a notable divergence in pedal travel between the vacuum and electro-hydraulic boosted brake systems, which the vacuum boosted system showing almost double the brake pedal travel of the electro-hydraulic brake system at 500 deg C initial brake temperature. This masking of increased fluid volume needed to pressurize the brake system that is apparent through pedal travel increase with the vacuum boosted brake system is the essential argument behind the "Fade Warning Assist" system. It is based on the premise that the increase in pedal force alone may not be sufficiently communicative of the state of the brake system to the driver.

The Fade Warning Assist feature essentially monitors what the driver cannot feel – the increasing fluid consumption of the brake system – and combines this with other predictive information to detect the onset of fade in the brake system and warn the driver. The details of how the feature works are proprietary to the companies that offer the feature. Two stages of fade warning are described in the owner's manual for GM vehicles so equipped [10]:

**FIGURE 2** Comparison of Average Pedal Forces and Travels for a high speed fade test, vacuum and electro-hydraulic brake actuation systems

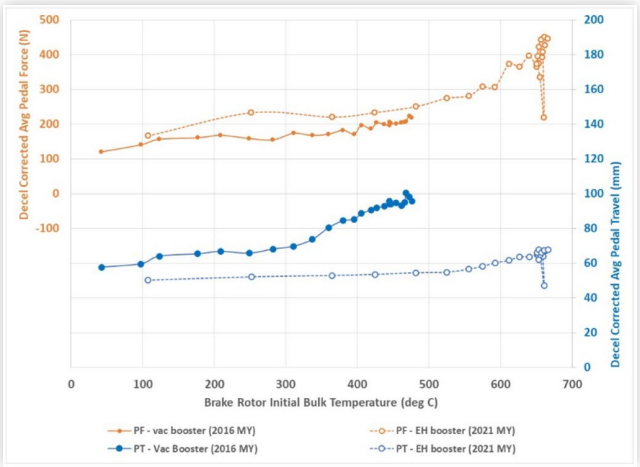


**Stage 1:** The Driver Information Center (DIC) displays a "Reduce Braking to Avoid Overheating" message and brake pedal effort and travel is increased. When the message displays, the driver should decrease brake pedal pressure.

**Stage 2:** The Driver Information Center (DIC) displays a "Brakes Overheated Service Now" message that the brake fluid temperature is excessive and is about to boil. The system increases brake pedal effort and travel and will also limit vehicle speed. The driver should immediately start a cool down lap if on the track. If this message displays, take the vehicle to be serviced at your dealer.

For purposes of illustration, a fictitious fade warning algorithm based on a simplified logic will be described in a later section.

## 2. Brake Corner Modeling – Raw Data

The sources of training data to represent the behavior of the front and rear brake corners in conditions ranging from "normal" operation on up into severe conditions in which fade occurs are inertia dynamometer-based tests designed specifically to map brake performance over this range. A test known as "fade envelope" starts in moderate (100 kph braking speed, 100 deg C initial brake disc temperature, 0.6g peak deceleration) conditions and extends into extremely severe use (up to 300 kph braking speed, up to 2.0g peak deceleration, and up to 700 deg C initial brake temperatures). The author acknowledges that the "moderate" condition is moderate only in the context of racetrack operation – 0.6g from 100 kph is already quite severe for public road driving. The conditions imparted by the test procedure start at the lowest temperature and map performance for a range of braking speeds and target deceleration levels, moves up to the next target initial brake temperature, and repeats the matrix of speeds and deceleration levels, and so on, which means that higher initial temperature stops have the effect of the history of the full range of speeds, deceleration levels, and lower initial temperatures before. Taper and cupping wear of the brake pads, and the effect of the braking history on the friction material itself will show up in the performance measured during the higher temperature sections of the test.

A 21" wheel envelope, 2-piece cast iron disc with aluminum hub, high performance brake corner with an aluminum 6-piston caliper and track-capable low-met (copper-free) brake pads was tested to provide training data for the machine learning model development. The recorded data were lightly processed to remove pre-and post braking event data and organized into a large rectangular matrix. Data were further processed to create new signals that could potentially have predictive power for the friction and fluid displacement outputs of interest.

It is noted here that it is typical best practice to normalize input and output data into the same range (such as -1 to 1). When working with many machine

learning models, such as neural networks, normalization can help make the training process more stable by getting everything into the same scale. In the present study, a comparison was made (this will be shown in a later section) between model performance with and without normalization. Very little difference was observed, possibly because the input data were already on a very similar scale; therefore, the data were not normalized for the rest of this study.

The recorded and calculated signals considered in the model development are summarized below, along with the rationale for considering each:

## 2.1. Temperature

Temperature is simultaneously one of the most intuitive predictors of brake performance, and one of the most complex and difficult to characterize. The brake pads and rotor, in operation, are almost never at a single temperature, but rather, they are the host of continually changing temperature gradients. At any given instant, temperatures almost certainly vary widely throughout the pad surface, the underlying pad matrix, and the disc surface. The bulk temperature of the brake disc – where temperature gradients tend to be the lowest – is commonly measured and then used to characterize brake performance which may actually be most strongly determined by temperatures at or near the friction surfaces. In other words, it is common practice to represent the "temperature" of the brake at any point in time as the temperature at the core of the disc. This was the case in the present study – brake rotor temperature was measured by a thermocouple embedded about halfway through the outboard plate of the disc.

Explaining the effect of temperature on the friction and wear of the brake involves a fair amount of generalizing. There is a pattern of behavior that can be related to the bulk temperature of the disc that is observable across a wide range of automotive friction materials, from non-asbestos organic to track-capable low metallic. As with most phenomena as complex as tribology, with so many competing effects at work, there is of course plenty of room for exceptions. A typical pattern is summarized and explained in figure 3:

## 2.2. Hydraulic Pressure

Hydraulic pressure is a strong predictor of clamp load that the caliper piston(s) impart to the adjacent brake pad(s). The compressive load on the brake pads can play a role in the pad to rotor friction – it has a strong effect on the pad to rotor pressure distributions and can be causally traced down to stresses on individual structural particles within the friction matrix and whether they dig in abrasively to the rotor surface or fracture. Figure 4 illustrates a qualitative relationship between pad to rotor coefficient of friction and clamp load. It should be noted here as well that increasing pressure in the caliper can shift the effective radius outward due to deflection of the caliper structure and shifting pressure distributions [8], which can either counteract the qualitative tribological effects depicted below:

**FIGURE 3** Qualitative relationship between friction in an automotive disc brake versus temperature

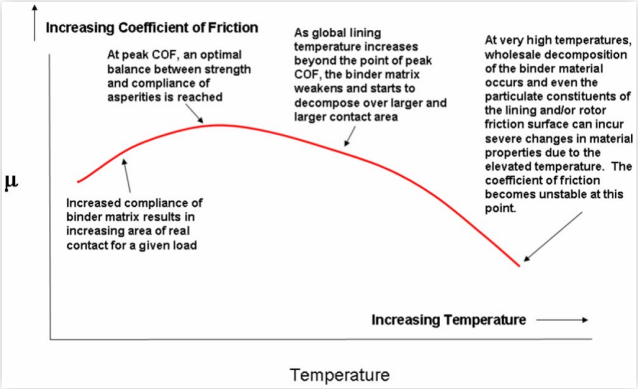


**FIGURE 4** Qualitative relationship between friction in an automotive disc brake and clamp load (pressure)

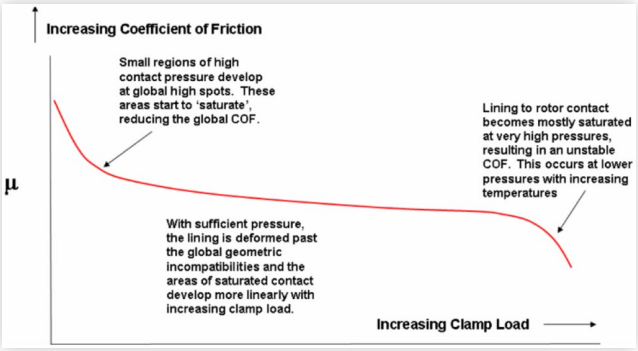


## 2.3. Rotational Speed

Rotational speed of the brake is concretely correlated with sliding speed at the tribological interfaces. Once again, there are competing effects at work that give rise to very interesting behavior (and once again, there is much room for exceptions when attempting to generalize this behavior). Automotive brake friction materials exhibit visco-elastic properties [11] and can generate friction by both adhesive and abrasive interactions with the counterface (the disc). At very high sliding speeds, the energy absorption of the brake can be quite high even at lower braking pressures, which can generate appreciable heating of the friction interface – in this respect, rotational speed and temperature (in this case, surface temperature) become strongly coupled. Figure 5 qualitatively describes the relationship between friction and sliding speed:

## 2.4. Instantaneous Braking Power

The power absorbed by the brake at every instant in time was calculated by multiplying the rotational speed signal

**FIGURE 5** Qualitative relationship between friction in an automotive disc brake and sliding speed.

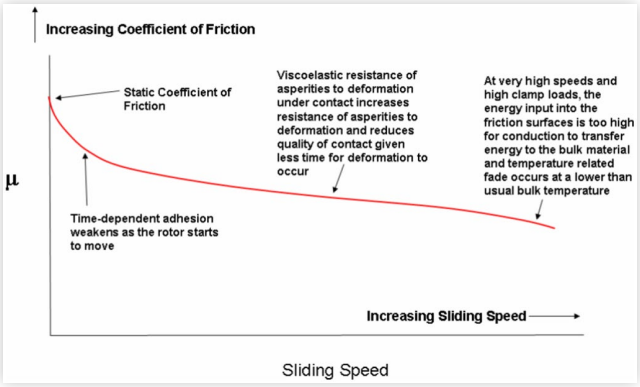


with the braking torque signal and expressed in units of kW. The theory behind the predictive power of this signal is that temperature gradients throughout the brake pads and the brake disc are driven by braking power. High braking power drives larger temperature gradients. Supplementing the measured disc bulk temperature signal with braking power in essence gives the machine learning model predictors that can be linked by physics to the temperature of the friction interface.

## 2.5. Cumulative In-Stop Work

A calculated parameter, cumulative in-stop work, was generated by integrating the braking power signal versus time. This signal was re-set to zero at the start of each braking event. The motivation for considering this signal was to give the machine learning models an input that captures recent braking history, at least to the extent of within the same braking event. Once brake fade sets in, the apparent friction versus time curve takes on a "bathtub" shape for most automotive friction materials, that can be marked by three phases [12]: (1) Initial braking, with a moderate friction level before the effect of massive power absorption and sharply increasing surface temperature takes hold, (2) in-stop fade, where the damage to the friction surface from absorbing sustained high braking power takes hold and friction decreases to a minimum, and (3) in-stop recovery, where braking speeds are lower, power is reduced, and ejection of hot wear debris and wear of the damaged surface reduce the friction interface temperature and allow it to be refreshed. The increase in apparent friction during the in-stop recovery phase may also be due to hysteresis in the brake, as the dynamometer will often be reducing pressure towards the end of the braking event. The hysteretic effect will exaggerate the apparent friction while pressure is being decreased.

Figure 6 shows the apparent friction of a 21" wheel envelope, front high performance brake, when braking from 200 kph at 1g with an initial temperature of 600 deg C:

The three phases of in-stop friction behavior are evident in this example. The hypothesis is that the cumulative in-stop work signal - and perhaps its interactions with the other predictors – can enable the machine learning models to capture some of this behavior.

**FIGURE 6** Apparent friction, temperature, and pressure of a high performance front brake during a 200 kph, 1g stop with 600 deg C initial temperature

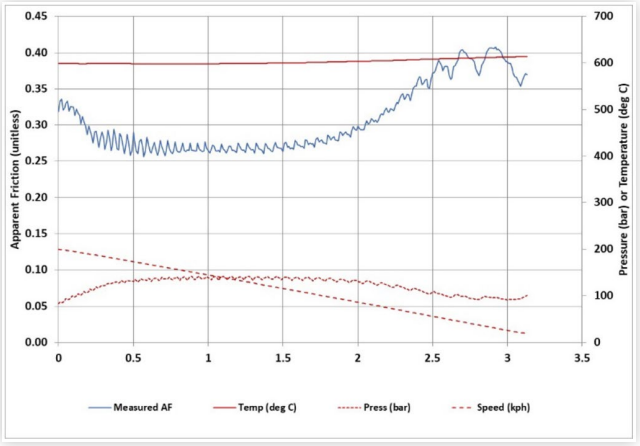


## 2.6. Total Cumulative Work on Friction Pair

Over the relatively short life of a brake friction set in racetrack conditions (measured in terms of laps of the track or tanks of fuel, rather than years or tens of thousands of miles), significant changes will occur. Taper wear, both in a radial direction and a tangential direction will be generated over repeated braking events, as will cupping wear under the pistons. These uneven wear patterns will decrease the mechanical efficiency of the caliper, shift the effective radii of the pad to rotor interfaces, and significantly affect the compliance of the brake corner [8]. Figure 7 shows the evolution of radial and

**FIGURE 7** Evolution of radial and tangential taper wear of inner and outer brake pads in a 6-piston high performance brake corner with track-capable low-met pads and cast iron disc during a high temperature wear test

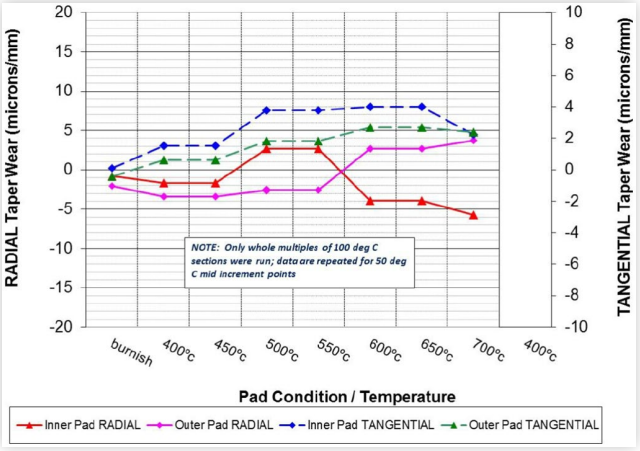

tangential taper wear for a high performance brake over the course of a high temperature wear test (with 50 stops per temperature block):

The hypothesis behind the predictive power of tracking cumulative energy absorbed by the friction set over its lifetime is that taper and cupping wear tracks to some extent with overall wear, and that as observed by past research, overall wear is strongly predicted by energy absorbed [13].

## 2.7. Target Signals

Two signals were identified to be the target of the machine learning models, one measured directly, and one calculated. Fluid displacement was measured directly by a flow meter on the brake inertia dynamometer and is a measure of how much brake fluid must be displaced into the brake corner in order to generate the desired pressure. In-vehicle, the brake actuation system must be able to displace enough fluid to pressurize all four brake corners to their respective target pressures (and note that target pressure is the same for each brake corner until tire traction limits are reached and proportioning and slip control take effect). The calculated parameter was apparent friction, which as defined in SAE J2784 [14], relates clamp load calculated from measured pressure and known piston area to brake friction force, calculated from torque and an approximate effective radius the friction force acts upon. Apparent friction allows the pressure required to produce the driver-intended amount of brake torque to be calculated.

Together, fluid displacement and apparent friction enable a thorough description of what the brake actuation, and ultimately the driver of the vehicle, must experience in order to brake the vehicle at the desired rate.

# 3. Machine Learning Model Development

As established in the previous section, six (6) potential predictor signals were gathered. Their selection was not accidental, it was curated based on the physics of operation of the brake corner and the potential to explain the observed behavior of the brake corner over the course of the previously described "fade envelope" test. It was also part of the model development strategy, knowing that machine learning models such as neural networks are "black box" models in which the relationships between the inputs and the outputs are so difficult to trace as to be effectively impossible to see – selecting inputs with strong physics-based rationale for their predictive power allows for some "sense check" of the model output to assure that it is generalizing appropriately.

Model development was done in a Matlab/Simulink® environment (2022a release), using both the *net fit tool* ("*nftool*") app and the *regression learner* app. The *regression learner* app allows the user to import predictor and target data and is configured to enable a wide variety of machine learning models to be quickly trained and evaluated. The *nftool* app allows the user to import predictor and target data as well but is focused solely on "shallow" neural networks (these are networks with with an input layer that collects the input signals and passes them directly to the hidden layer, only one hidden layer, which processes the data through activation and weighting functions, and an output layer, that further modifies the data and collects it into one or more output signals). It has features that allow for trained models to easily be productionized in code or as a Simulink® block. Models were evaluated to predict apparent friction, and separate models were developed to predict fluid displacement.

The initial experimentation phase of model development, using the *regression learner* app, is not the primary focus of this paper, so only a concise summary is offered. After trying a large range of combinations of input signals and model types, shallow neural network models, and fine decision tree models both performed well (about equivalently so). Deep neural networks (with two hidden layers) performed marginally better than the shallow, but not enough to justify the added complexity. There are numerous sources online in which researchers compare and contrast neural networks and decision trees, many lauding the understandability of the decision trees. One researcher [15] went as far as to prove that any neural network can be equivalently represented by a decision tree. Ultimately, the author chose to focus on shallow neural networks, due to their high performance, to past success in using them for similar work, and to the seamless productionization into a form that is easily implemented into system-level models.

Further work concentrated on shallow neural networks, trained in the Matlab® *nftool* app. Figure 8 summarizes some of the model configurations that were trained to predict apparent friction, and their resultant performance. In all cases, data were separated into groups of 70% training data, 15% validation data, and 15% test data. Note that only 5 of the 6 predictor signals that were prepared were used for apparent friction modeling (total cumulative energy absorbed was used for the displacement predictions):

Model 5 is highlighted because it was the highest performing and was selected for further validation of friction behavior. Models 5 and 7 differed only in the respect that the input and output data for model 7 were

**FIGURE 8** Summary of Select Shallow Neural Network Model Configurations and Performance for prediction of apparent friction during "fade envelope" test

| Model # | Press | Temp | Speed | Cum Work | Power | Hidden Layer | $R^2$ | MSE |
|---|---|---|---|---|---|---|---|---|
| 1 | | x | x | x | x | 10 neurons | 0.8427 | 0.001300 |
| 2 | | x | x | x | x | 20 neurons | 0.8681 | 0.001100 |
| 3 | x | x | x | | | 10 neurons | 0.8675 | 0.001100 |
| 4 | x | x | x | x | | 10 neurons | 0.8925 | 0.000900 |
| 5 | x | x | x | x | x | 10 neurons | 0.9995 | 0.000004 |
| 6 | | x | x | x | | 6 neurons | 0.7968 | 0.001700 |
| 7 | x (N) | x (N) | x (N) | x (N) | x (N) pwr | 10 neurons | 0.9973 | 0.000214 |

*N = normalized to range of -1 to +1*

normalized to a range of -1 to +1 before training. The slight difference in performance (in favour of model 5 for which the data were not normalized) is likely due to the stochastic learning process in which the initial weights are randomly seeded; this allows for some variation in the resultant model from training session to training session, even when working with the same data.

Comparing models 1 and 2, for which the size of the hidden layer was doubled but inputs were kept the same, only a modest boost in performance was attained with the large increase in hidden layer size. Model 6 was configured similarly to the models used previously by the author [2], with one key difference being that the in the previous work, data were sampled in increments of 1 kph change in speed, while in the present study data were sampled at a full 100 Hz – this may have allowed the earlier model to generalize more effectively.

Inclusion of pressure as a predictor was a source of some debate in the project team. As summarized in the section 2.2, there are solid physics based reasons for pressure to have an influence on the tribology of the friction interface. However, pressure is also the direct result of friction changing when controlling to a deceleration or torque target. In the training data, the decrease in friction and the subsequent increase in pressure as fade set in is already there in the recorded history the data represents. After deploying in a brake system model and running different braking conditions that what was included in the fade envelope test, there is an appreciable risk that strong interactions between pressure and the other signals may allow good model performance so long as the braking conditions are identical or very similar to those in the test but then cause strongly divergent performance in the different vehicle test simulation conditions. It will be shown in the next section that this turned out to be true, to a strong extent.

Figure 9 summarizes select model configurations that were trained to predict fluid displacement during the fade envelope test.

Every model for fluid consumption included pressure because fluid consumption is essentially driven by the stresses on the brake corner caused by fluid pressure. Comparing models 3 and 4, it may be seen that adding in the total cumulative work signal – potentially indicative of the more slowly evolving (e.g., slower than within a single braking event) taper wear and cupping wear conditions – significantly enhances model performance, reducing mean squared error in model 4 to a third of that of model 3.

**FIGURE 9** Summary of Select Shallow Neural Network Model Configurations and Performance for prediction of fluid displacement during "fade envelope" test

| Model | Press | Temp | Speed | Cum Work | Power | Total Cum Work | Hidden Layer | $R^2$ | MSE |
|---|---|---|---|---|---|---|---|---|---|
| 1 | X | x | | | | | 10 neurons | 0.8427 | 1.068 |
| 2 | x | x | | x | | | 10 neurons | 0.8928 | 0.8278 |
| 3 | x | x | x | x | x | | 20 neurons | 0.9232 | 0.6140 |
| 4 | x | x | x | x | x | x | 20 neurons | 0.9751 | 0.2005 |

In developing the preferred models, summary statistics such as the correlation coefficient and mean squared error were used for comparison. However, to ensure that the models were adequately describing the most critical behaviors of the physical parts, the modeled and measured data were also studied graphically. Critical behaviors included capturing the in-stop fade behavior correctly and adjusting realistically for very high or very low power stops. The full extent of graphical data examined is overly cumbersome to convey in paper; instead, a curated selection of graphical comparisons is shown.

Figure 10 shows model 5 output vs. measured data for a 100 deg C initial brake temperature (IBT), 100 kph stop at 1g on the top panel, a 300 deg C IBT, 200 kph, 1g stop in the middle panel, and a 600 deg C IBT, 300 kph, 1g stop in the lower panel:

As one might expect from a 99.99% correlation coefficient, the neural network modeled apparent friction is more or less on top of the measured data in virtually all braking conditions of the test. The source of the odd fluctuation in apparent friction in the 300 kph, 600 deg C stop is unknown. The apparent friction fluctuation is likely due to the pressure fluctuation, which in turn may have been a dynamometer control issue; as pressure was more or less saturated against the 180 bar programmed limit and control issues could have arose when in-stop wear caused a reduction of pressure and subsequent compensation by the dynamometer.

Figure 11 shows the predictions of fluid displacement model 4 versus the measured data for the same braking conditions shown in figure 10 (100 deg C IBT, 100 kph, 1g top panel, 300 deg C IBT, 200 kph, 1g middle panel, and 600 deg C IBT, 300 kph, 1g lower panel).

As summarized in figure 11, measured and modeled fluid displacement tracked well across a very wide range of operating conditions.

## 4. Validation with New Braking Conditions (and Model Refinement)

The newly trained neural network models for apparent friction and for fluid displacement prediction (for the 21" wheel envelope, 6-piston caliper high performance brake corner that has been the object of research to this point) were implemented in a Simulink® environment. New braking conditions were generated by a vehicle level simulation to represent a General Motors straight line brake fade test procedure, with scalable braking speed and braking intervals to match the braking severity of any target racetrack for that vehicle. The speeds and cycle time were set to represent the braking severity that would be seen by a 650 hp sport sedan running fast laps at Virginia International Raceway (VIR). Brake snubs from

**FIGURE 10** HP 6-piston, cast iron disc front brake corner NN modeled (grey line) vs. measured (blue line) apparent friction during select stops from Fade Envelope test. NN with pressure, temperature, speed, cumulative work, and power as inputs

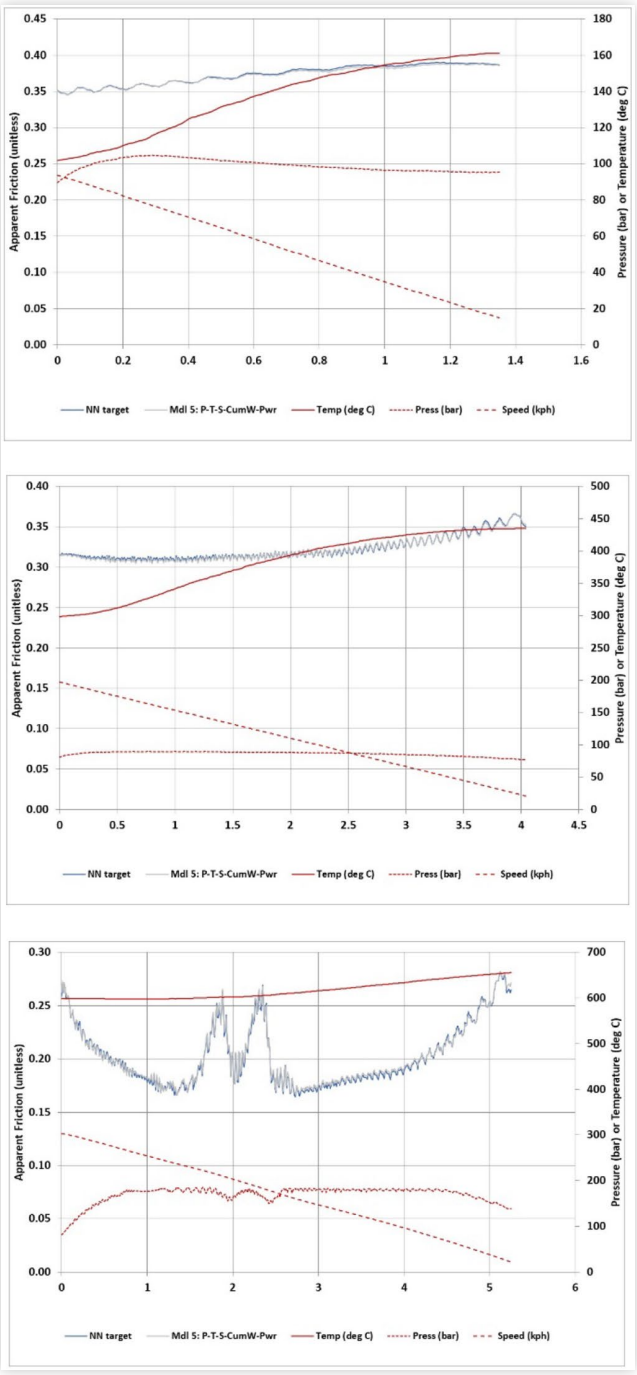


230 kph down to 50 kph were repeated at intervals of approximately 24 seconds.

For this initial test of the brake corner model, the signals from the vehicle level model (pressure, temperature, and speed) were recorded and played back into the brake corner model to observe torque and fluid displacement. Figure 12 summarizes the output of the two neural networks, representing the brake corner model. The

**FIGURE 11** HP 6-piston, cast iron disc front brake corner NN modeled (grey line) vs. measured (blue line) fluid displacement during select stops from Fade Envelope test

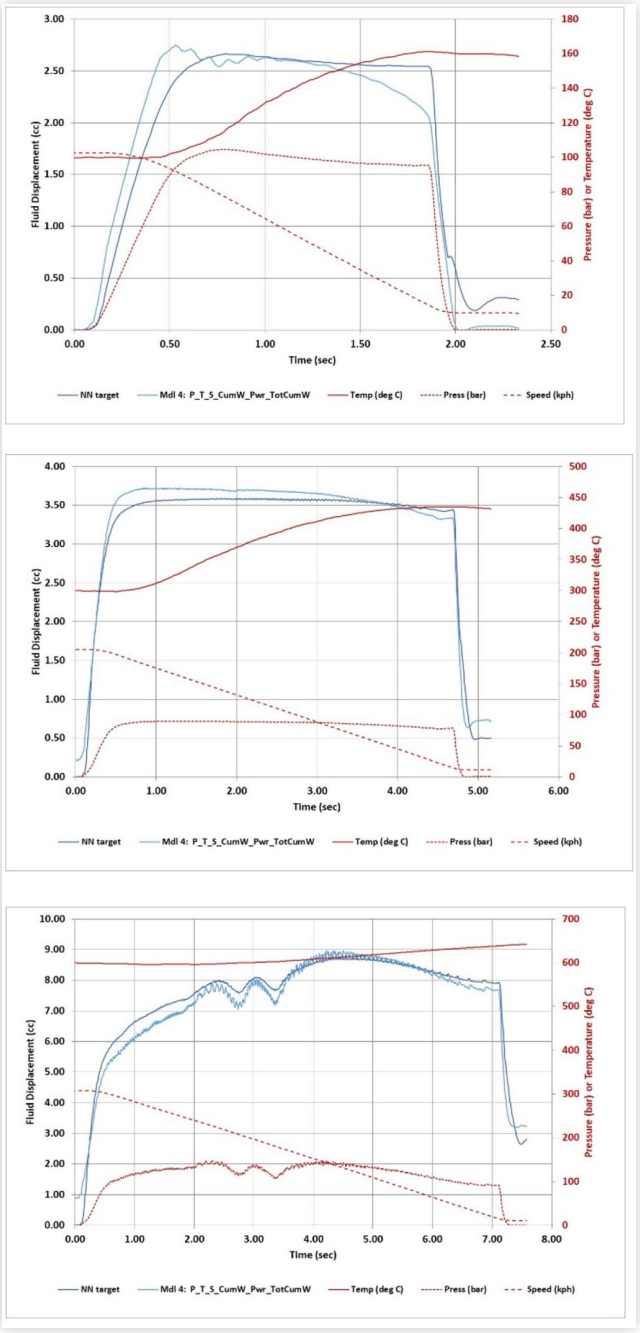


apparent friction was converted into torque using the pressure signal and the appropriate geometry-based transformations (such as effective radius and piston area).

The torque for a single front brake corner should have been an order of magnitude higher for this test (in excess of 2000 Nm), but the predictions were generally less than 100 Nm peak. The fluid displacement prediction went negative when off-brake, which brought to forefront the point that when integrated into a system model, the brake corner neural net model would need to be sampled only when the brakes are applied, and their output should

**FIGURE 12** Initial brake corner model output during simulation of flat track test with comparable braking severity to Virginia International Raceway (Model 5 for apparent friction/torque, Model 4 for fluid displacement)

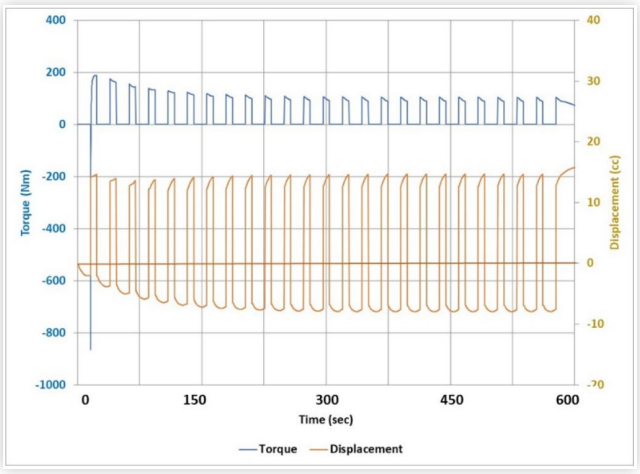


be suppressed (force to zero) when the brakes are released. This is easily remedied in the system model, however, a deeper concern that the fluid displacement peaks were really not changing much over the test (where initial brake temperatures rose from ambient to over 500 deg C).

The dramatic shift in model output when fed input data from braking conditions that were not explicitly contained in test used to generate training data suggested that while the models generalized well within the test conditions it was explicitly trained with – they did not generalize well when faced with slightly different conditions. It is possible that the model instability in the "off" brake condition affected the logic for re-setting the braking event dependent inputs such as cumulative work, and this resulted in an unrealistic mis-match of inputs even for the new braking conditions, but a combination of time constraints and general concern over model stability led to change in direction in model development.

A second round of model development took place, with the goal of preserving as much of the accuracy achieved by the first models as possible, but creating models that would generalize better when faced with braking conditions that are in between those explicitly contained in the training data (it was never a goal to create models that would extend outside of the range of the training data, as this becomes risky for virtually all machine learning model types; this is why the fade envelope test has such a wide range of braking conditions). Two key hypotheses informed the subsequent round of model development. First, that the potentially unstable feedback loop of using pressure to predict apparent friction (caused by increasing pressure generally causing lower friction to be predicted, requiring more pressure and therefore lowering the friction prediction even further) would need to be eliminated. Second, for fluid displacement – pressure would remain a critical predictor, but training data that exercised the brake over the entire pressure range should be used. During the fade stops, pressure would be ramped in very quickly to reach the target torque (decel) level quickly, and very little data would be recorded during the pressure rise compared to the "hold" portion of the event. The test did incorporate series of "ramp" applies, where pressure is ramped up linearly to a cutoff pressure (about 130 bar). These ramp applies were placed immediately after each temperature block of the fade test, which enabled the ramp applies to be performed at each temperature increment of the test.

A new, simpler neural network model for apparent friction was trained using Temperature, Speed, Cumulative Work, and Power as inputs. Again, a shallow network architecture was used, with 6 neurons in the hidden layer. Training data was from the fade stops from the fade envelope test. Figure 13 shows the summary statistics and regression of measured vs. predicted value for this network:

It is reasonable to take note of the slope of the modeled vs. measured data (0.71); this suggests that on average the model predicts apparent frictin that is 29% lower than the actual. Close study of the data stop by stop (not shown here) indicated that the model was generalizing well for mid to high energy braking events and mid to high temperature braking events. Much of the under-prediction was for the lower temperature (100

**FIGURE 13** Summary statistics and actual vs. predicted regression models for Neural Network to predict apparent friction of brake corner during fade test using Temperature, Speed, Cumulative Work, and Power.

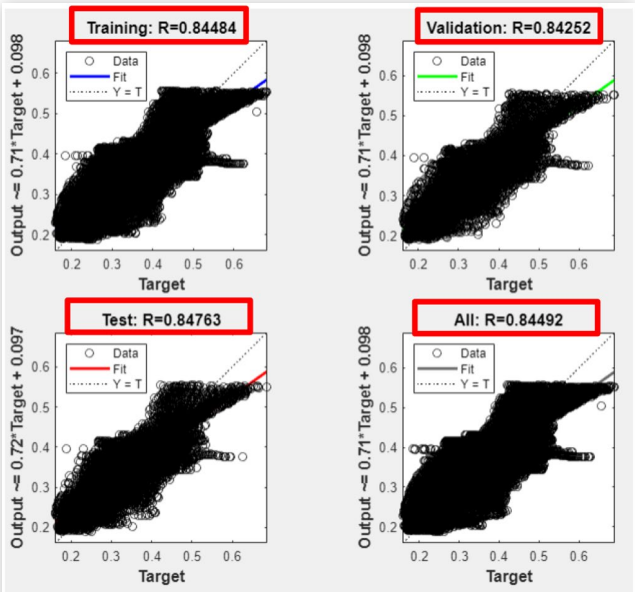


| | Observations | MSE | R |
|---|---|---|---|
| Training | 194156 | 0.0013 | 0.8448 |
| Validation | 41605 | 0.0013 | 0.8425 |
| Test | 41605 | 0.0013 | 0.8476 |

and 200 deg C) braking events. The model also tended to under-predict apparent friction towards the end of the stop, where the hysteretic effects that occur as pressure is reduced artificially raise the apparent friction (due to actual clamp load in the system being higher than what is calculated by pressure and piston area alone). Similarly, if one looks at the summary statistics for the validation data and takes, for example, an actual value of apparent friction of 0.40 – one would note that the model predicts anywere from 0.22 to 0.50. By looking at the time-history measured and modeled data in a similar fashion, it becomes evident that the bulk of the descrepancy occurs in the least critical portion of the braking events where extraction of the apparent friction value even in the measured data meets with some difficulty, namely the very onset of braking and the hysteretic portion at the end of the event. This underscores the importance raised earlier of looking beyond the summary statistics and validating that the model is doing well what it needs to do well, and accepting when needed comprimise when it is not critical to the objectives of the model. The author will editorialize briefly – it is especially true when working with "black box" models such as neural networks to document the validation of the model and make clear what applications are is scope of its capabilities and where it may be limited.

Figure 14 shows the three curated braking events shown previously for the other models (100 deg C IBT, 100 kph, 1g top panel, 300 deg C IBT, 200 kph, 1g center panel, and 600 deg C, 300 kph, 1g bottom panel):

Importantly, even with the reduced fidelity, the model for apparent friction was still predicting the critical onset of braking to mid-stop with good fidelity. The most significant divergence of the model and measured data were during the less critical "recovery" phase towards the end of the stop.

For fluid displacement, the training data were switched to the ramp stops done after each temperature block of the fade test. This allowed for a more equal representation of the working pressure range of the brake system in the data. Model development was done in four steps:

1. Linear-exponential regression models of the form:

$$Disp = \left(1 - e^{-c \cdot Press}\right) \cdot \left(K \cdot Press + b\right)$$

Where c, K, and b are regression coefficients, were fitted to the data at each temperature level.

2. The fitted models were used to estimate fluid displacement across the entire working pressure range of the brake system (0 to 180 bar)
3. Two models were developed in parallel to interpolate the resulting data for pressure and temperature. One was a linear interpolation, which essentially realized the final model as a two-dimensional lookup table, mapping pressure and temperature to fluid displacement. The other was a shallow neural network with only 3 neurons in the hidden layer, to interpolate between pressure and temperature.
4. The ramp applies were all lower speed (100 kph initial), and we terminated upon reaching the pressure limit. Therefore, little if any in-stop behavior could be represented. By studying the lower panel of figure 11, one may see that fluid displacement increases around t=4.0 seconds,

**FIGURE 14** HP 6-piston, cast iron disc front brake corner NN modeled (gold line) vs. measured (blue line) apparent friction during select stops from Fade Envelope test. NN with temperature, speed, cumulative work, and power as inputs

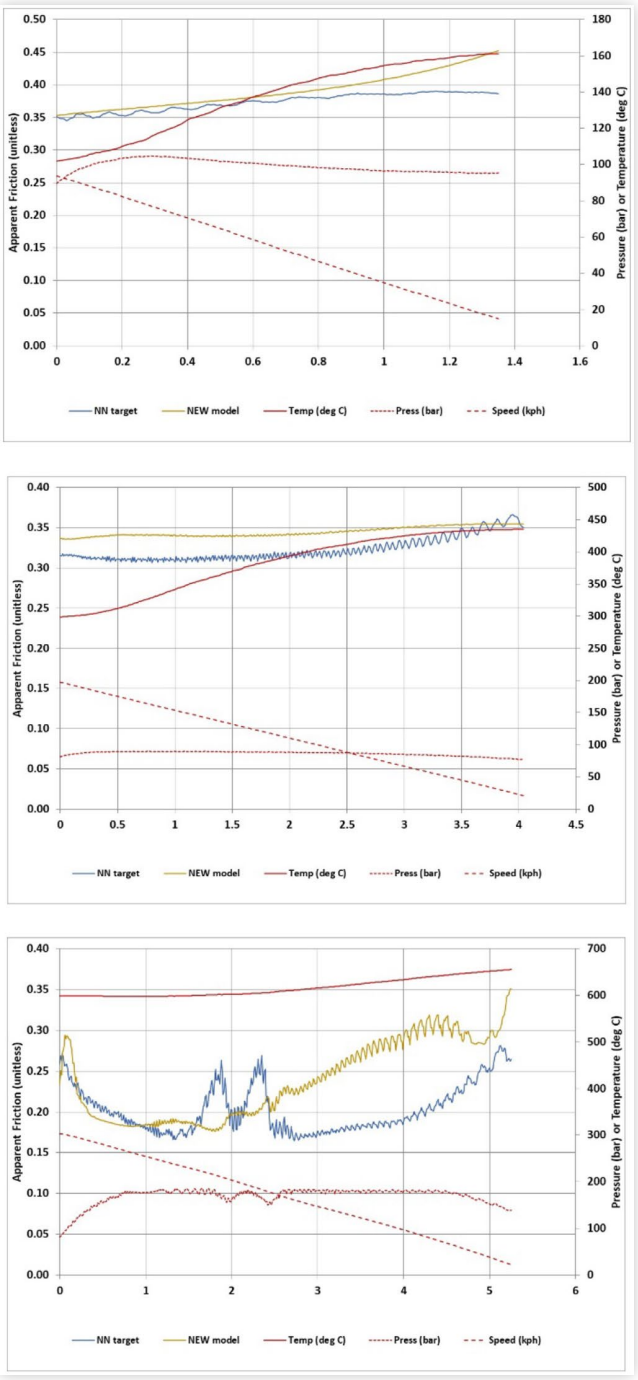

while pressure holds steady. The hypothesis was formed that the physics of this behavior are explainable in significant part through in-stop wear that occurs during very high energy braking conditions, and that it could be predicted by adding a real-time, high-energy wear model and adding the in-stop wear predicted by the model to the fluid displacement prediction. It had been established in earlier work [16] that even in racetrack conditions, wear can be adequately represented with a specific wear versus temperature lookup table (specific wear is a measure of volumetric wear of the friction material per unit energy absorbed by the brake). The present work expanded on this by adding a modifier to the wear rate based on braking power (wear will generally increase as braking power/intensity increases, and vice versa). The wear rate modifier was based on wear testing at different braking power levels within the same initial brake temperature block.

Further evidence of the physics behind point number 4 above were present in the displacement to pressure hysteresis characteristic of the brake corner. Figure 15 shows fluid displacement versus pressure for a high energy stop (250 kph initial braking speed) for the subject high performance front brake corner:

Of interest in figure 15 is the "flat edge" on the right hand edge of the loop – this is where the pressure limit set for the dynamometer was reached. 180 bar pressure was held, but fluid displacement increased by over 1cc while pressure remained constant. This can be attributed to the combined effects of in-stop wear, and in-stop heating. Both effects are captured in the revised fluid displacement model. It is likely that viscoelastic creep of the pad and insulator under high compressive forces contribute to this as well, however these effects are generally on the order of tens of microns [17] and would contribute only about 0.03cc per ten microns of creep (far less than the almost 2 cc effect observed).

Figure 16 shows the revised brake corner model output when exercised during the same flat-track test

**FIGURE 15** Fluid Displacement vs. Pressure hysteresis loop during 250 kph, 600 deg C IBT braking event

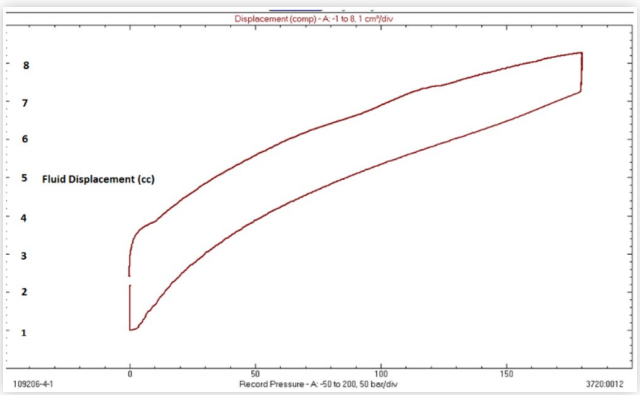


**FIGURE 16** Revised brake corner model output during simulation of flat track test with comparable braking severity to Virginia International Raceway (NN trained with temperature, speed, cumulative work, and power for apparent friction, and both 2d lookup table and NN based displacement estimate)

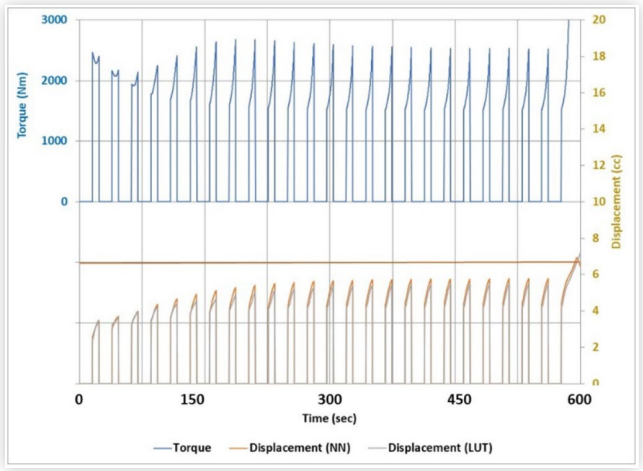


simulating Virginia International Raceway severity braking as in figure 12:

The behavior of the model as the fade test progresses and brake temperatures increase is much more intuitive. Note that the test data had a repeating pressure cycle for each brake event (the pressure profile was the same from brake event to brake event); the variation in torque and fluid displacement was caused solely by the changing temperature of the brake and the interaction of temperature with the other model inputs (speed, cumulative work, and power).

## 5. System Model and Model Predictions

A rear brake corner model was created following the same process by which the front brake corner model was created. The rear brake corner model was based on a 4-piston opposed, aluminum caliper with a full-cast iron disc and track-capable low met (copper free) brake pads. The front and rear brake corner models were combined into a system level model within a Simulink® environment. Brake thermal behavior was represented by proven lumped capacitance models [2]. For test purposes, a slip control was modeled with simple behavioral models only; however, the brake corner models were designed to integrate easily into commercial vehicle dynamics analysis software such as CarSim™ that can further integrate with Hardware In the Loop or Software In the Loop to provide much higher fidelity representations of slip control.

Two vehicle configurations were modeled – one was the same 650 hp sport sedan that the brake corner models were tested with. The other was the same vehicle,

with the peak propulsion power increased to 1000 hp (a modification made quite easy by the virtual environment). The second configuration was intended to ensure that the brake system would be "stressed" to the point of appreciable fade. Both of the vehicle with full brake system models were exercised over the previously described flat track test with braking severity aligned to Virginia International Raceway. Figure set 17 shows brake pedal force, travel, and temperature (top panel) and brake pressures and full brake system fluid consumption (lower panel) over the 25 stop test:

Figure set 18 depicts the same for the 1,000 hp "fast" configuration:

The baseline run reached initial brake temperatures (IBTs) of about 573 deg C on the front brake and 506 deg C on the rear. Brake pedal force, travel, pressure, and fluid displacement all follow an intuitively expected pattern as the test progresses and brake temperature reaches pseudo-equilibrium. The test conditions in figure 2 were slightly different than what was simulated (speeds, cycle time, and resultant temperatures were slightly different), but comparing the stabilized pedal force and travel at a common IBT of 570 deg C, the modeled and measured

**FIGURE 17** Full Vehicle Model Predictions of Brake Pedal Force, Travel and Front Disc Temperature (top panel), Brake Pressures and Fluid Consumption (lower panel) during flat-track simulated session at VIR – "baseline" 650 hp vehicle

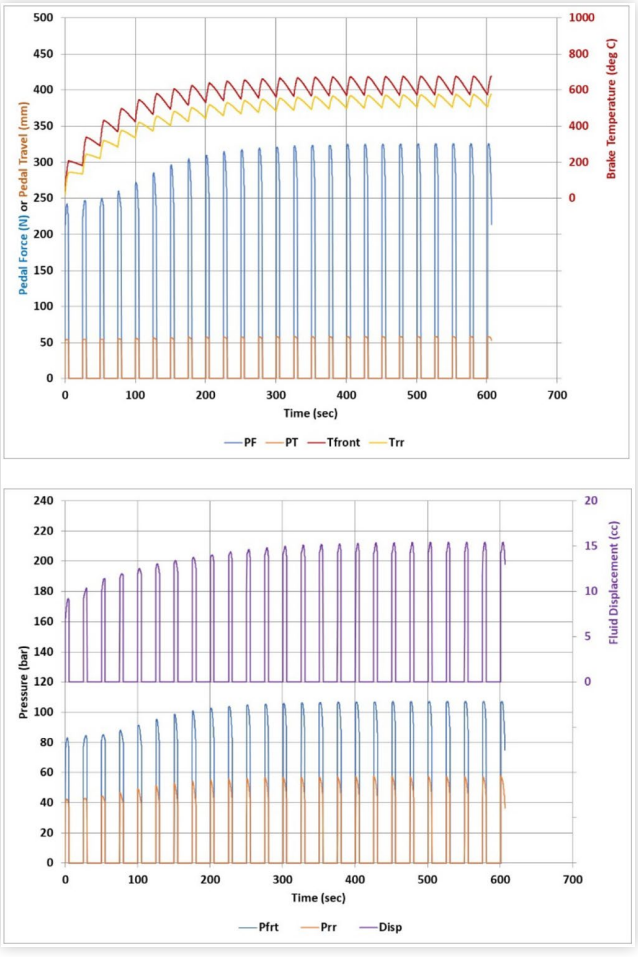


**FIGURE 18** Full Vehicle Model Predictions of Brake Pedal Force, Travel and Front Disc Temperature (top panel), Brake Pressures and Fluid Consumption (lower panel) during flat-track simulated session at VIR – "fast" 1,000 hp vehicle

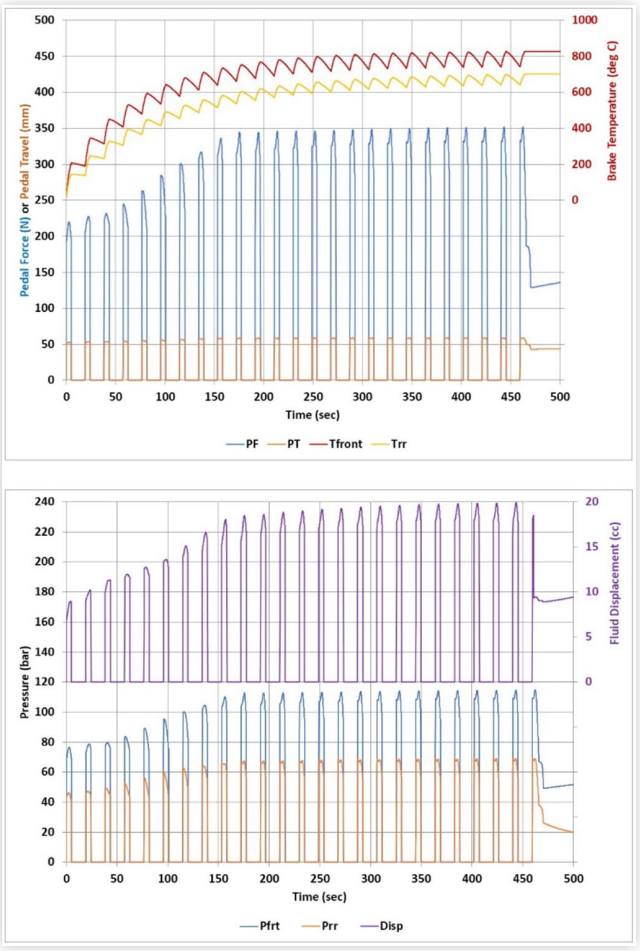


results compare favorably (pedal force was 305N in physical vehicle test and about 326N in the slightly higher energy simulation, while pedal travel was about 58mm in both). The differences were within normal pedal feel simulator variation. Brake system fluid displacement reached about 15 cc at 1g.

The 1,000 hp configuration saw IBT increase to 741 deg C on the front and 641 deg C on the rear. Stabilized pedal forces were 352N; travel was 59mm. Perhaps most noticeably – brake system fluid displacement increased to 19 cc at 1g.

Sufficient data were generated at this point to circle back now to one of the original motivations of this work – calibrating and predicting the operation of Fade Warning features. Although the detailed logic by which the stages of fade warning are triggered are proprietary to suppliers and OEM's that have developed them, there are some general principles that are common, and for purposes of the present study, can be represented in a simplified, behavioral manner. State of the art algorithms (at least at the time of the present work) monitor brake system fluid consumption – measured fairly precisely by the travel of the internal hydraulic plunger

that pressurizes the brake system – and compare observed degradation (added fluid volume at a given pressure level in the system) versus a baseline "normal" curve. They may also factor in some measure of brake system output, such as a "wheel lock pressure."

A simple fade warning algorithm – not necessarily aligned with actual algorithms in use today – is summarized here, for purposes of this study. In this hypothetical, highly simplified algorithm, brake fade may be triggered by either of two "paths." In the first, brake system fluid displacement is compared continuously to calibrated limits. A baseline "volume vs. pressure" curve represents normal operation. A second curve, set a calibratable fixed volume above the baseline, can trigger the first level of fade warning. A third curve, set a calibratable fixed volume above the baseline curve (always higher volume that the first curve), can trigger the second level of fade warning. In the second path, the "wheel lock pressure" is calculated based on measured wheel slip and pressure. If wheel lock pressure exceeds a calibratable value (one for each level of fade warning), then the warning may be triggered by this path. It should be noted that once a vehicle enters slip control such as Anti-Lock Brakes, control valves are cycled, and pressure releases occur, it becomes very difficult to impossible for the brake actuation unit to keep track of fluid displacement. For this reason, a fluid displacement-based trigger for fade warning will generally be suppressed once slip control is activated; however, this is precisely the point at which a wheel locking pressure based trigger becomes the most accurate. In this manner, good coverage may be achieved by this simplified algorithm for fade detection. Other influences such as knock-back and pry back of brake calipers during sessions with high lateral acceleration or rough road inputs can confound the compliance-based detection, however, this complexity is beyond the scope of the present work.

An initial set of calibrations were set – for purposes of illustration, they were set conservatively, with level 1 fade warning setting with 4cc increase and 120 bar locking pressure, and level 2 setting with an 8cc increase and 140 bar locking pressure.

Figure set 19 summarizes these metrics for the lower powered baseline vehicle. The top panel shows the brake system fluid displacement versus pressure for each of the snubs in the fade test; the lower panel summarizes the locking pressure. The corresponding initial calibrations are shown in each of the panels (fluid displacement limits in the top panel; locking pressure limits in the lower panel):

It is readily apparent in both panels of figure set 19 that level 1 fade warning is triggered by both paths (and it is set during snub #7 by both). The front brake initial temperature is about 500 deg C at this point. It is worth addressing the interesting shape of the displacement plots in the top panel of figure set 19 – the curvature after peak pressure is reached and it starts to decrease again. This is the in-stop heating and wear effects in the model, with shared explanation in physics to the displacement-pressure hysteresis curve measured on the inertia dynamometer (figure 15). As noted earlier, if the curved "tail" of the displacement curves in figure set 19 occur after slip control activation, this portion of the curve may not be considered in the detection of fade. After setting fade warning level 1, performance of the brake system stabilizes and fade level 2 is never set.

**FIGURE 19** Brake System Compliance(top panel) and Front Brake Wheel Locking Pressure (lower panel) during Fade Test, baseline 650 hp vehicle

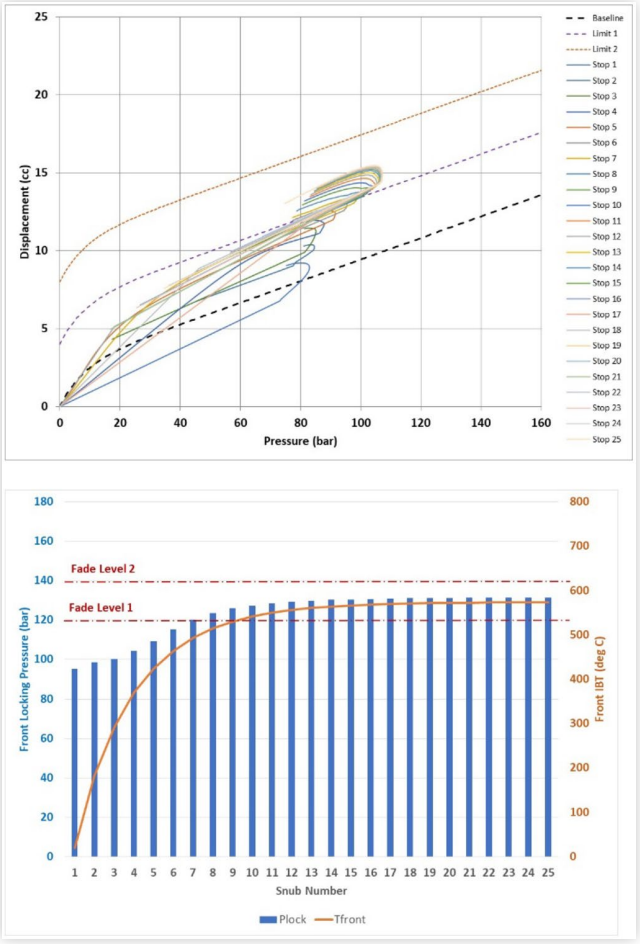


Figure Set 20 shows the same for the "fast" 1,000 hp configuration:

In the case of the "fast" vehicle configuration, fade warning level 1 is set by the fluid displacement trigger path during snub #5, and then fade warning level 2 is set by the locking pressure trigger path during snub #9.

Although increased fade as a result of adding 350 hp to a vehicle's propulsion without improving the brake system is thoroughly unsurprising to most brake engineers, it is fair to question whether setting a fade warning by snub number 7 (equivalent in energy to about 2-3 laps of VIR) is really necessary, given the relatively high performance level at which the brake system stabilized. The initial calibrations – already acknowledged as conservative – were revised. The new thresholds were +5cc for fade level 1, and +10cc for fade level 2, with a wheel lock pressure threshold of 140 bar for fade level 1 and 160 bar for fade level 2. These new settings result in no fade warning for the baseline vehicle. The "fast" configuration sets fade warning level 1 during snub #6.

**FIGURE 20** Brake System Compliance(top panel) and Front Brake Wheel Locking Pressure (lower panel) during Fade Test, "fast" 1,000 hp vehicle

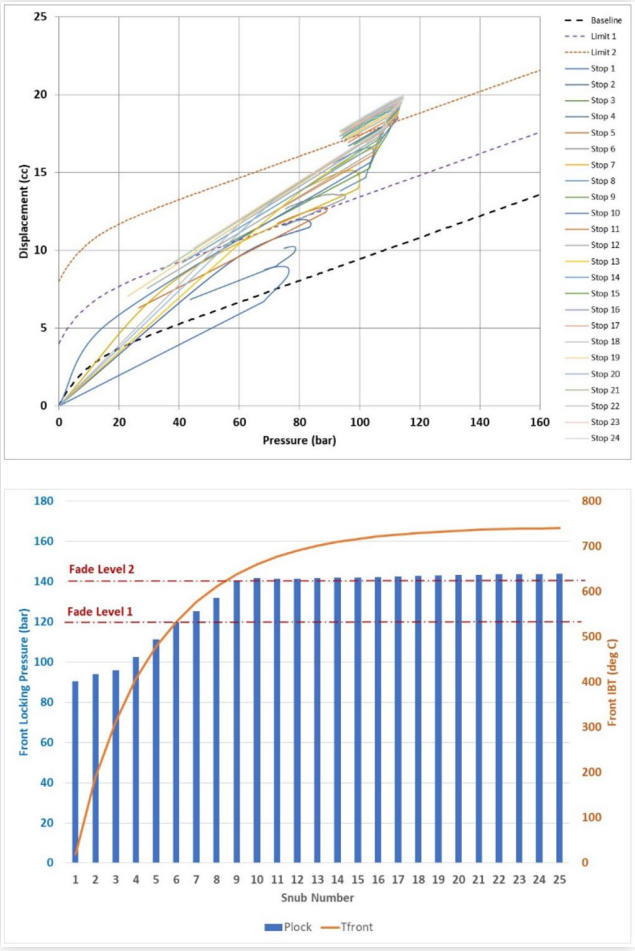


**FIGURE 21** Predicted Front and Rear Brake Pad Wear during Fade Test, both baseline and "fast" vehicle configurations shown

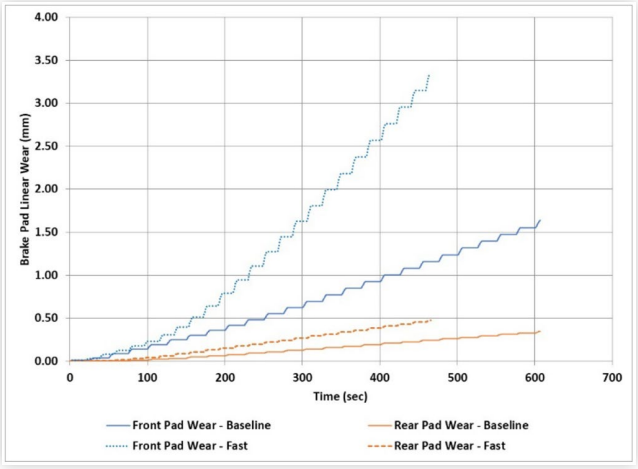


It is informative to check the predicted brake pad wear; as both wear and friction result from the tribological conditions in the braking interfaces. An argument can be made to tune the fade warning such that it is also protecting against rapid wear-out. Figure 21 summarizes the front and rear brake pad wear during the fade schedule for both the baseline and "fast" configurations:

The "fast" configuration exhibited front pad wear roughly 3 times higher than the baseline. While the baseline front pads could be expected to last through 3-4 tanks of fuel, the fast configuration would potentially not last more than 1. Considering the projected pad wear rates, the revised fade warning calibration that displays warning for the "fast" configuration but leaves the driver alone for the baseline gains credibility.

# Summary/Conclusions

With the motivation of developing vehicle level models equipped with brake systems of sufficient fidelity to represent the complex, in-stop varying behavior that can occur during high energy driving scenarios, machine-learning based brake corner models were developed and successfully integrated into the brake system. An initial goal of the work was to explore of useful system integration work could be done on such a model and tuning of the "fade warning" feature inherent in many vehicles equipped with modern electro-hydraulic brake by wire apply systems was selected as the focus of the present research. Initial efforts to develop brake corner models for friction and fluid displacement used neural network models for both. Models were trained using data from a single-ended inertia dynamometer fade test that was designed to map brake corner performance versus temperature, deceleration level, and speed. The initial efforts achieved very high correlation coefficients and low mean squared error with training, test, and validation data sets using pressure, temperature, speed, cumulative in-stop work, and power as predictors (with total cumulative work on the friction added for the displacement model). However, when exposed to new braking patterns outside of the specific stop conditions in the dynamometer test, some model instabilities were observed. The models were revised, removing braking pressure as a predictor for friction, and switching to a lookup table plus wear model to represent fluid consumption. The revised models displaced stable, credible behavior.

The new brake corner models were integrated into a brake system level model for a high performance sport sedan; a baseline 650 hp and a fictitious 1,000 hp variant were both represented. The vehicle models were exercised over a flat-track fade scheduled designed to represent the braking severity of Virginia International Raceway. A basic "fade warning" algorithm logic was described, and it was demonstrated that the data from the vehicle model equipped with the machine learning brake corner models could usefully inform the calibration of this feature.

# Future Work

The next level of functionality to represent brake corner behavior with enough fidelity to support high quality vehicle integration, including tuning of controls and features, would be to faithfully capture the hysteretic effects that occur when the brake is applied and released. As this kind of cycling is central to slip control features, representing the brake corner behavior accurately in these conditions is important to enable their tuning and integration. Hysteresis is caused by friction in the brake – piston(s) to bore(s), guide pins to bores (if so equipped), and pads to abutments. It can also be caused by changing pad to rotor friction in-stop. Another rich vein of research opportunity lies in application of machine learning to predicting integration effects for a friction pair – for example, an appropriate model can predict the performance of a brake corner after making design changes, or even a new brake corner entirely by using surrogate measured data and detailed physics-based modeling of the conditions at the friction interface. Given the vast complexity of friction behavior, the power of machine learning once again provides a tempting path to improve current state of the art.

# References


1. Barber, A., "Accurate Models for Complex Vehicle Components using Empirical Methods," SAE Technical Paper 2000-01-1625 (2000), https://doi.org/10.4271/2000-01-1625.
2. Antanaitis, D., Nisonger, R., and Riefe, M., "Prediction of Brake System Performance during Race Track/High Energy Driving Conditions with Integrated Vehicle Dynamics and Neural-Network Subsystem Models," SAE Technical Paper 2009-01-0860 (2009), https://doi.org/10.4271/2009-01-0860.
3. Satapathy, B.K. and Bijwe, J., "Performance of Friction Materials based on Variation in Nature of Organic Fibres Part 1. Fade and Recovery Behavior," *Wear* 257 (2004): 573-584, doi:10.1016/j.wear.20045.03.003.
4. Rhee, S.K., Jacko, M.G., and Tsang, P.H.S., "The Role of Friction Film in Friction, Wear and Noise of Automotive Brakes," *Wear* (1991): 89-97.
5. Ostermeyer, G.P., "On the Dynamics of the Friction Coefficient," *Sear* (2003): 852-858, doi:10.1016/S0043-1648(03)00235-7.
6. Aledsendric, D., et. al., "Prediction of Brake Friction Materials Recovery Performance Using Artificial Neural Networks," *Tribology International* (2010), doi:10.1016/j.triboint.2010.05.013.
7. Travagliati, A., "Novel Modelling Techniques of the Evolution of the Brake Friction in Disc Brakes for Automotive Applications," SAE Technical Paper 2020-01-1621 (2020), https://doi.org/10.4271/2020-01-1621.
8. Antanaitis, D. and Sanford, J., "The Effect of Racetrack / High Energy Driving on Brake Caliper Performance," SAE Technical Paper 2006-01-0472 (2001), https://doi.org/10.4271/2006-01-0472.
9. Antanaitis, D., "Measuring and Characterizing Brake System Performance During Racetrack / High Energy Driving Conditions," SAE Technical Paper 2005-01-0790 (2005), https://doi.org/10.4271/2005-01-0790.
10. 2020 Chevrolet Corvette Owner's Manual, "Track Events and Competitive Driving" section, "Brake Fade Warning Assist" subsection.
11. Newcomb, T.P. and Spurr, R.T., "Friction Materials for Brakes," *Journal of Tribology* (1971): 75-81.
12. Antanaitis, D., Monsere, P., and Riefe, M., ""Brake System and Subsystem Design Considerations for Racetrack and High Energy Usage Based on Fade Limits," SAE Int," *J. Passeng. Cars - Mech. Syst.* 1, no. 1 (2009): 689-708, https://doi.org/10.4271/2008-01-0817.
13. Liu, T. and Rhee, S.K., "High Temperature Wear of Semimetallic Disc Brake Pads," *Wear* 46 (1978): 213-218.
14. SAE Surface Vehicle Recommend Practice J2784, FMVSS Inertia Dynamometer Test Procedure for Vehicles Below 4540 kg GVWR, January 27, 2021, SAE International.
15. Aytekin, C., *Neural Networks are Decision Trees* (Cornell University, 2022). https://doi.org/10.48550/arXiv.2210.05189
16. Antanaitis, D., "Methods for Sizing Brake Pads for High Performance Brakes," *SAE Int. J. Mater. Manf.* 9, no. 1 (2016), https://doi.org/10.4271/2015-01-2679.
17. Agudelo, C., Hamann, K.., Abendroth, H.., Gente, C.., Giese, A.., "Improvements to Laboratory Compressibility Measurements and New Application Areas", Eurobrake Paper EB2012-TM-19RE, 2012, FISITA.


## Acknowledgments

The author gratefully acknowledges the contributions of Lee Harder, Dr. Heewook Lee, Cara Learman, and Chris Morgan, all of General Motors Product Engineering.

## Definitions/Abbreviations

**DIC** - Driver Information Center
**FWA** - Fade Warning Algorithm
**HIL** - Hardware In the Loop
**IBT** - Initial Brake Temperature
**OEM** - Original Equipment Manufacturer
**SIL** - Software In the Loop
**VIR** - Virginia International Raceway



e-ISSN 2641-9645